2019

Evaporation-Driven Micromixing in Sessile Droplets for Miniaturized Absorbance-Based Colorimetry

A. Chandramohan
Purdue University

M. Chakraborty
Indian Institute of Technology Kharagpur

J. A. Weibel
Purdue University, jaweibel@purdue.edu

S V. Garimella
University of Vermont, sureshg@purdue.edu

Chandramohan, A.; Chakraborty, M.; Weibel, J. A.; and Garimella, S V., "Evaporation-Driven Micromixing in Sessile Droplets for Miniaturized Absorbance-Based Colorimetry" (2019). *CTRC Research Publications.* Paper 350.
http://dx.doi.org/10.1021/acsomega.9b02784

ACS OMEGA

Article

Cite This: ACS Omega 2019, 4, 22385−22391

http://pubs.acs.org/journal/acsodf

Evaporation-Driven Micromixing in Sessile Droplets for Miniaturized Absorbance-Based Colorimetry

Aditya Chandramohan, Monojit Chakraborty,[†] Justin A. Weibel, and Suresh V. Garimella*[,‡]

School of Mechanical Engineering and Birck Nanotechnology Center, Purdue University, West Lafayette, Indiana 47907, United States

Supporting Information

ABSTRACT: We demonstrate the use of an evaporating, sessile droplet on a nonwetting substrate as a miniature micromixing device to conduct sample−dye reactions for absorbance-based colorimetry. The nonwetting substrate supports buoyancy-induced mixing inside the droplet for rapid completion of the measurement. The Bradford assay is used as a proof of concept, where a protein-containing sample is reacted with a reagent dye to measure the protein concentration. Viability of absorbance measurement through the droplet is first established using droplets in which the reactants are mixed prior to their deposition onto the substrate. In a second set of experiments involving in situ mixing, the reagent is directly added to a sessile droplet of the protein-containing sample, allowing the reactants to mix while the absorbance is being measured. Interplay between buoyancy-induced mixing, protein−reagent reaction, and protein adsorption onto the substrate leads to a complex temporal absorbance measurement signal. Videos corresponding to the signal data show that each of these mechanisms dominates during different phases of droplet evolution, causing a signal pattern containing peaks and valleys having a strong monotonic trend with the protein concentration. Overall, the second absorbance peak at which the reaction nears completion is the most sensitive to sample concentration. Heating of the substrate is demonstrated to dramatically speed up the mixing process. These protein concentration measurements, obtained with a simpler system and low reactant volumes, demonstrate that this droplet micromixing concept is a viable alternative to microtiter plates for colorimetric applications.

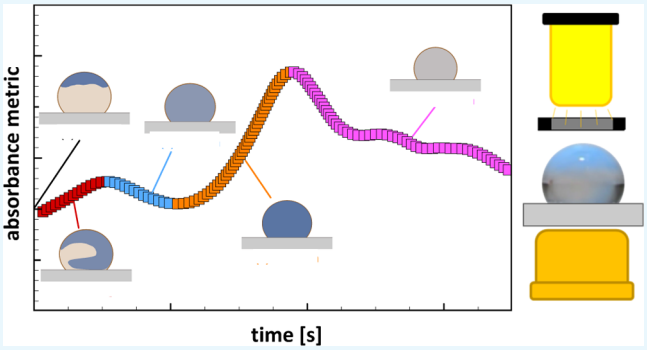

1. INTRODUCTION

Colorimetry is a widely used approach for measurement of the concentration of biological samples in a liquid. Colorimetry techniques have been developed to detect concentrations of glucose,[1] protein,[2−4] fatty acids,[5] nucleic acids,[6] and so forth. In colorimetry, the sample is mixed with a reagent that causes a color change in the sample−reagent mixture that is a function of the concentration of the sample. Conventional colorimetric analysis involves measuring the mixture absorbance at a specific wavelength using either a colorimeter, spectrophotometer, or microtiter plate reader.[7] Miniaturization of this process has the benefits of reducing the quantity of the reagent and the sample needed, thus allowing for less invasive testing in clinical applications. The measurement time can also be significantly reduced because of the faster mixing process in miniaturized systems.

The Bradford assay is one of the most commonly used protein quantitation techniques. The technique involves mixing a protein-containing sample with the reagent dye Coomassie Brilliant Blue G-250. This reagent dye is known to exist in three ionic states: anionic, cationic, and neutral.[8] The neutral and anionic states both react to the amino acids in the protein, the former by hydrophobic and electrostatic interactions and the latter by electrostatic interactions.[9] These reactions form protein−dye complexes that shift the absorbance spectrum of the mixture. The measured absorbance change is correlated with a set of standard concentrations to determine the protein concentration in the sample.[2] The noninstantaneous nature of this protein−dye reaction means that there is likely a combined effect of the reaction and the mixing on the signal during the measurement timescale. In conventional Bradford assays that are conducted in macroscale cuvettes, the measurement requires on the order of 5 min for the reaction to be completed[7] because of the longer time for mixing in macroscale devices. Macroscale mixing can also lead to protein denaturation and foaming with excessive vortexing.[10] A quicker method of mixing that avoids denaturation, as is possible at the smaller length scales of micromixing techniques, can allow the reaction to be completed more rapidly.

Several techniques for miniaturized colorimetry have been presented in the literature, with microfluidic electrowetting-on-

Received: August 28, 2019
Accepted: November 18, 2019
Published: December 18, 2019

dielectric (EWOD) devices[11] and paper-based devices[12] representing a majority of the efforts. Some devices rely on EWOD as an actuation method for transporting droplets to a sensor.[11,13] This approach typically involves use of a hydrophobic substrate to ease droplet transport. A process of shuttling the droplet is utilized to ensure mixing of the sample and reagent. A significant challenge from the use of hydrophobic substrates is the irreversible adsorption of hydrophobic proteins onto the substrate, causing contamination of the sample and device.[14] This is often mitigated by using oil as a separation layer.[15] Paper-based microfluidic devices rely on capillary action to drive the fluids.[12] This approach provides the benefit of low-cost, passively-driven flow. Some of the limitations of using this approach for colorimetry include low sample flow efficiency, potential for leakage, and inability to measure extremely low concentrations.[16] An alternative, sessile droplet-based technique was recently demonstrated for a hue-based colorimetry system that relies on measuring the color of the sample using an imaging system.[17] Absorbance-based colorimetry, which is required for many commonly used techniques like the Bradford and Lowry assays, has not been previously explored using sessile droplets.

Recent efforts have attempted high-throughput screening of sample concentration using absorbance-based colorimetry by fabricating miniaturized wells with higher density of wells per unit area than previously achieved;[18] however, these techniques require complex machining to create precise wells at such high density. Furthermore, a key issue that must be addressed in these low-volume microwells is the thorough mixing of the samples.[19] Several active micromixing approaches have been proposed in the literature, including ultrasonication,[20] external vibration of T-junction microchannels,[21] magnetohydrodynamic stirrers,[22] and electroosmotic flow in microchannels.[23] Most of these approaches demand complex control schemes and additional manufacturing requirements. Multilaminar mixing is another approach that uses intricate patterns of channels to induce chaotic flows.[24] This technique often requires longer flow lengths[21] and still requires complex fabrication to create the complex flow patterns necessary for mixing. A simpler micromixing system could thus benefit high-throughput microplate-based colorimetric analysis.

Several characteristics of droplets placed on nonwetting surfaces make such surfaces an attractive platform for miniaturized colorimetry. Droplets on nonwetting surfaces demonstrate significantly lower evaporation rates than droplets on wetting substrates[25] because of the suppression of evaporation at the contact line of the droplet due to vapor confinement[25] combined with evaporative cooling.[26,27] This suppression is an important feature for colorimetric applications, where the reaction needs to be completed and the absorbance measurement taken before too much evaporation has occurred. Furthermore, aqueous droplets demonstrate buoyancy-driven convection on nonwetting substrates,[28] which offers an order of magnitude higher internal flow velocities[28] compared to wetting surfaces.[29] This leads to buoyancy-induced mixing rates that are two orders of magnitude higher than simple diffusion-based mixing,[28] without requiring long flow lengths as in other passive micromixers. This aspect of the droplet-based system reduces the time to complete the reaction between the dye and the reagent. Finally, sessile droplets of known volumes and contact angles can be simply placed on a hydrophobic substrate with a small footprint, without the need for complex fabrication of microplates.

Based on the concepts described above, we propose a technique that would use a droplet microarray as an alternative to microtiter plates for absorbance-based colorimetry. The concept involves making real-time absorbance measurements through droplets on a nonwetting substrate, where the droplets are formed by placing a droplet of the reagent dye upon a droplet of sample solution, and comparing the absorbance signal response to that of standards. These standards are several prepared samples with known concentrations that exceed the expected range of the test case concentrations. The nonwetting substrate induces buoyancy-driven convection and ensures rapid mixing and complete reaction of the reagent into the sample, while also ensuring that evaporation of the droplet is suppressed. The absorbance is measured by illuminating the droplet at the wavelength of interest from one side and measuring the outgoing light on the other. The current study demonstrates this sessile-droplet-based absorbance measurement for colorimetric analysis of protein concentration. A proof of concept implementation approach is described, and real-time absorbance measurement signals are analyzed for premixed droplets and in situ droplet mixing.

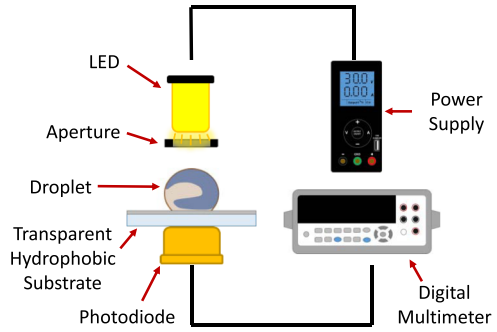

Figure 1. Schematic diagram of the sessile-droplet-based absorbance measurement.

2. MATERIALS AND METHODS

Figure 1 shows a schematic diagram of the experimental setup used for the absorbance measurements. The setup detects the light transmitted through a sessile droplet placed on a transparent, nonwetting substrate. An InGaAlP light-emitting diode (LED) with a peak wavelength of 590 ± 10 nm (LED591E, Thorlabs) is aligned with a silicon photodiode (FD11A, Thorlabs) through a 0.84 mm-diameter aperture that confines the area of illumination to within the radius of the droplet base footprint. The photodiode, which has a wavelength range of 320−1100 nm, is connected to a digital multimeter (34410A, Keysight) that records the signal at 10 Hz using a LabVIEW interface. The nonwetting substrate is fabricated using a glass slide of 1 mm thickness (3057, Gold Seal). The slide is cut into a 25 mm × 25 mm square substrate and cleaned in succession with acetone, methanol, and deionized (DI) water. Teflon granules (Teflon AF2400, Dupont) are dissolved in a solvent (Fluorinert Electronic Liquid FC-72, 3M) to create a 1% weight/volume solution. This solution is then spin-coated onto clean glass at 1500 rpm. The coated slides are then baked on a hot plate at 150 °C for 2 h. The resulting low-surface-energy surface exhibits a contact angle of 125° for the sample−reagent mixture used in the

DOI: 10.1021/acsomega.9b02784
ACS Omega 2019, 4, 22385−22391

experiments. It should be noted that protein irreversibly adsorbs onto hydrophobic surfaces, making these surfaces single-use at a specific location.

The droplet is composed of two solutions: the sample and the reagent. The sample is prepared by dissolving standard bovine serum albumin (98% lyophilized powder, Sigma-Aldrich) into DI water to achieve the desired concentration of protein; the sample concentration is defined in the rest of this work by the amount of protein in DI water. The reagent is the Bradford reagent mixture (Sigma-Aldrich), which contains Coomassie Brilliant Blue G-250 dye in phosphoric acid and methanol. The reagent is initially of a reddish-brown color. The reaction between the protein (in the sample) and dye (in the reagent) results in the liquid changing to a blue color, with the degree of change corresponding to the concentration of protein in the sample. The change in absorbance of the liquid is most sensitive at a wavelength near 590 nm.

Experiments are conducted in two different configurations: (1) a premixed case to confirm that the absorbance signals measured through the droplet medium have a detectable change over the target range of sample concentrations and (2) an in situ mixing case to demonstrate the proposed concept of using the droplet as a self-contained passive mixing apparatus to make colorimetric measurements. All of the aforementioned experiments are performed at room temperature (21.5 °C) and both the sample and reagent are filtered before the experiments. For the premixed case, the sample and reagent are thoroughly mixed in a sample to reagent ratio of 1:5 in a test tube. After the sample is thoroughly mixed and the reaction is complete, a 10 μL droplet of this mixture is deposited on the substrate, quickly aligned between the LED and photodiode, and the signal recorded in volts. This approach effectively measures the signal of the completely reacted mixture, without introducing the complexities of real-time mixing and any reactions within the droplet. For the in situ mixing case, a 1.7 μL droplet of the sample is first placed on the nonwetting substrate. The reagent in the amount of 8.3 μL is then added to the sample droplet, thereby creating an approximately 1:5 sample to reagent ratio. The droplet is then aligned with the photodiode and the signal measured in real time for 1000 s. The experiments for both configurations are conducted at three sample concentrations: 0.1 mg/mL (1.51 μM), 0.15 mg/mL (2.26 μM), and 0.3 mg/mL (4.51 μM). These were selected to avoid the saturation effects that are present in the Bradford assay at higher concentrations and limit protein aggregation. Three trials are conducted at each sample concentration to ensure repeatability. Three additional trials are performed at a concentration of 0.15 mg/mL (2.26 μM) with the substrate heated to 40 °C to demonstrate acceleration of the mixing process at elevated temperatures.

In order to calculate an absorbance metric from the raw signal, a "blank" sample is used for reference, as is the case in conventional colorimetry. A droplet of a sample without protein (0 mg/mL concentration) is used as the blank, which allows a reference signal to be measured that takes into account the curvature of the droplet and the resulting lensing effects. Use of a blank sample for reference in this manner is possible because the pinned evaporation characteristics of the blank sample droplets are nearly identical to those of droplets with protein samples, as confirmed by the goniometric measurements shown in Figure S1 of the Supporting Information; the volume and height evolution of the droplets with and without protein in the sample during evaporation are identical. A key

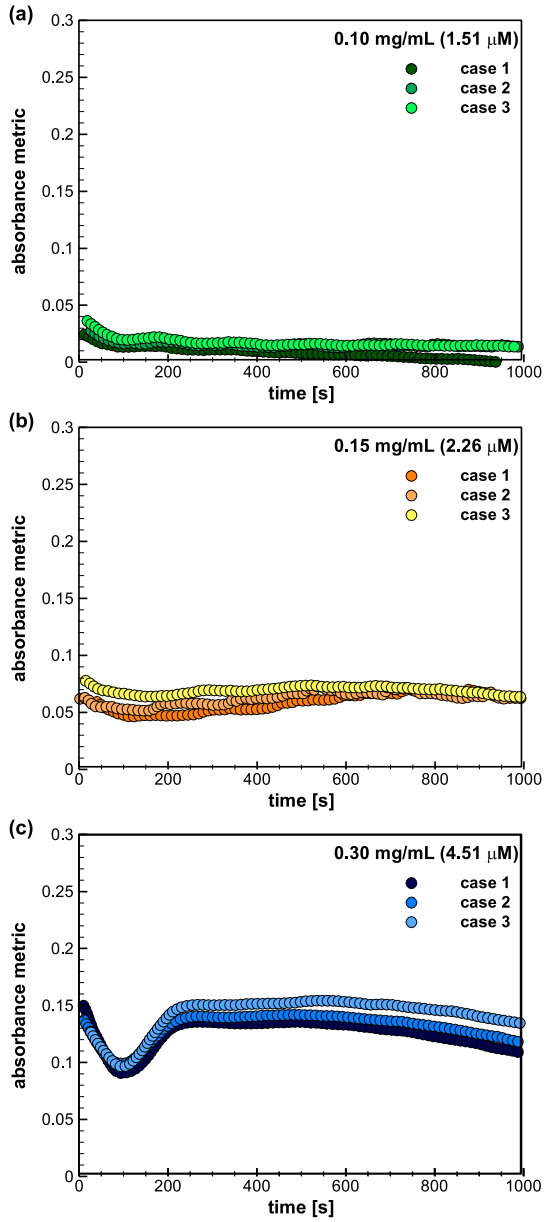

Figure 2. Time-resolved absorbance measurements for premixed sample droplets at concentrations of (a) 1.51, (b) 2.26, and (c) 4.51 μM.

assumption in the absorbance metric is that the intensity of light incident on the photodiode is linearly proportional to the voltage signal output read by the multimeter. Based on this assumption, a formulation analogous to Beer's law is used to calculate the absorbance metric

$$A = \log_{10}\left(\frac{V_0}{V}\right)$$

where A is the absorbance metric, V_o is the voltage reading from the blank sample, and V is the voltage reading from the sample that is being measured. The signal measured from the blank sample is relatively constant throughout evaporation at a mean value of 0.1303 V. The overall lack of change in the signal with evaporation indicates that any changes in lensing with changes in droplet volume are negligible with respect to the measured absorbance signal. As the sample concentration increases, it is expected that the absorbance signal at the LED

DOI: 10.1021/acsomega.9b02784
ACS Omega 2019, 4, 22385−22391

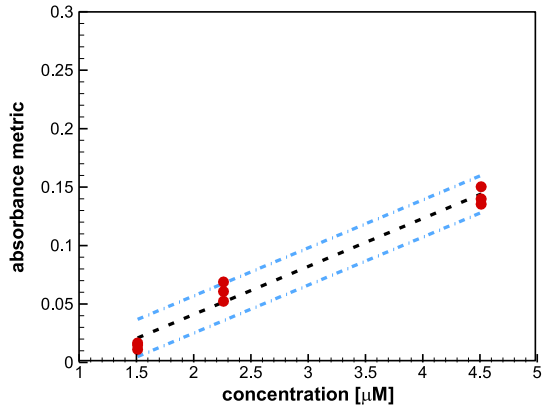

Figure 3. Absorbance metric values for the sample at 400 s (extracted from Figure 2) plotted as a function of concentration, along with a linear fit (dashed line) and an 80% prediction interval (dash-dotted line).

will increase (i.e., the raw voltage signal will decrease) because of the liquid color change.

3. RESULTS AND DISCUSSION

Figure 2 shows the absorbance metric measurements for premixed sample concentrations of 0.1 mg/mL (1.51 μM), 0.15 mg/mL (2.26 μM), and 0.3 mg/mL (4.51 μM). The raw voltage measurements that were used to calculate these values are provided for reference in Figure S2 of the Supporting Information. As can be clearly seen in Figure 2, the absorbance generally increases with concentration. There is an initial valley in the absorbance signal that becomes more pronounced at higher concentrations. This valley is likely due to buoyant convection in the droplet initially mixing the components and temporarily diluting the protein faster than it can react. There is also a gradual monotonic decrease in the absorbance with time toward the end of the measurement period as the protein absorbs onto the Teflon-coated substrate, reducing the droplet concentration. This trend is more apparent with increasing concentration because of the higher contrast in the signal between the blank and the test samples. Figure 3 shows the absorbance metric value at 400 s as a function of the sample concentration, with a linear fit and an 80% prediction interval. A strong monotonic increase in absorbance is observed with increasing concentration. With this experimental confirmation of a measurable trend in the absorbance for a sessile droplet configuration, the proposed method of mixing in situ without resorting to an external mixing apparatus is explored next.

The in situ mixing absorbance measurements, at sample concentrations of 0.1 mg/mL (1.51 μM), 0.15 mg/mL (2.26 μM), and 0.3 mg/mL (4.51 μM), are shown in Figure 4a–c, respectively. Raw signal measurements for these test cases are included in Figure S3 of the Supporting Information. A complex temporal absorbance signal is recorded for all samples, consistently featuring a slight increase followed by a slight decrease and then a large increase (approximately within the first ~400 s). Lastly, there is a gradual monotonic decrease in the absorbance metric that continues to the end of the experiment. This signal evolution results in two initial absorbance metric peaks (local maxima) with a valley (local minimum) in between. Overall, the absorbance increases with increasing protein concentration, as was observed in the

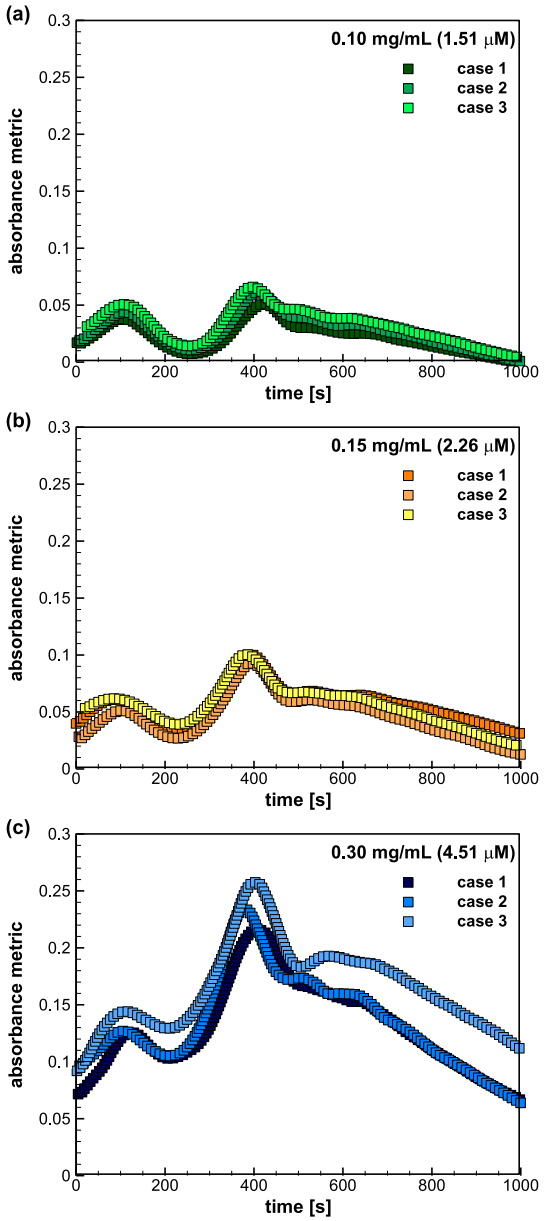

Figure 4. Time-resolved absorbance measurements for in situ mixed droplets at sample concentrations of (a) 1.51, (b) 2.26, and (c) 4.51 μM.

premixed cases; this concentration dependence is especially prominent for the peak and valley values.

To understand the complexities of this evolution, videos were collected during the mixing and reaction process for the sample droplet of concentration 0.3 mg/mL (4.51 μM). At this concentration, color changes due to the reaction are clearly observable in the visible spectrum. A camera is placed horizontally facing the droplet to obtain a simultaneous record through the time period of the absorbance measurement. Images extracted from this video at 100 s increments are shown in Figure 5. The images illustrate the interplay of buoyancy-induced mixing, chemical reaction, and protein adsorption, which play a significant role in determining the signal measured through the droplet as it progresses through multiple color levels of darker blue (higher absorbance at the 590 nm wavelength) and lighter blue or brown (lower absorbance at the 590 nm wavelength). Alongside the

DOI: 10.1021/acsomega.9b02784
ACS Omega 2019, 4, 22385−22391

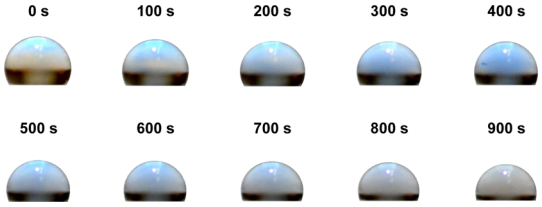

Figure 5. Image frames, captured at 100 s increments from the droplet video (available in the Supporting Information) for the in situ mixing case at a concentration of 0.3 mg/mL (4.51 μM). The image background outside the droplet profile is cropped for clarity.

discussion to follow, the reader is encouraged to view the videos included as the Supporting Information, which best illustrate this progression.

The color distribution observed in the video is analyzed to determine the dominant mechanisms that lead to the different phases of the droplet temporal absorbance signal. These phases are determined by observing the peaks and valleys, and the trends in-between, in the absorbance metric plot shown in Figure 4c. The phases and associated mechanisms are illustrated in the representative inset diagrams of Figure 6:

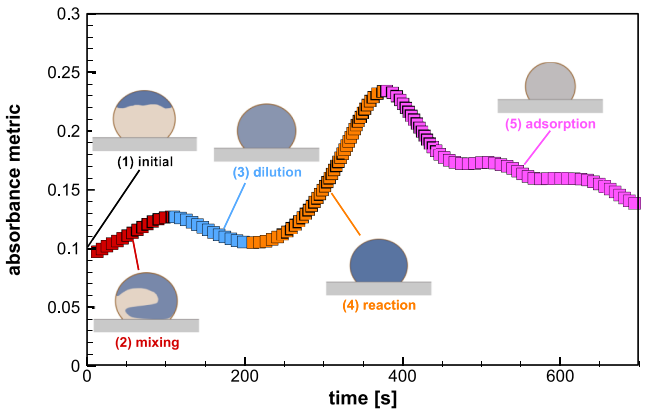

Figure 6. Plot of the temporal absorbance metric for a selected trial at a sample concentration of 0.3 mg/mL (4.51 μM) with inset schematic drawings showing the various phases of in situ mixing of the reactant and sample, including: (1) the initial droplet, (2) the mixing phase, (3) the dilution phase, (4) the reaction phase, and (5) the adsorption phase.

(1) Initially, the protein sample amasses at the top of the droplet and the initial reaction creates a dark blue region directly in the path between the light source and the photodiode. Buoyant convection then distributes this mass through the droplet in the subsequent (2) mixing phase, causing more of the protein to react and resulting in the absorbance increasing slightly during this phase. However, the mixing eventually dilutes the color faster than the reaction occurs in the (3) dilution phase, resulting in the droplet absorbance decreasing slightly. Once the sample is thoroughly mixed, the droplet enters a (4) reaction phase where the reaction dominates dilution, thus darkening the droplet and increasing the absorbance dramatically. Once most of the protein has reacted into protein−dye complexes, the droplet enters the (5) adsorption phase, where the protein adsorbs onto the Teflon-coated substrate faster than any continuing reaction. This causes the droplet to revert to the native reddish-brown color of the reagent, and the absorbance metric drops monotonically till the end of the experiment. The time difference between the two peaks in the absorbance signal was analyzed and found to be virtually identical across all concentrations (293.3 ± 12.9 s), indicating that the mixing and reaction time scales do not change discernibly with concentration. This is expected as the substrate temperature is held constant in all the trials, resulting in the same extent of buoyancy-induced convection.

Figure 7 shows an analysis of the measured absorbance metric at the peaks and valley. The values for the first peak, the valley, and the second peak are plotted as a function of concentration in Figure 7a−c along with a linear fit and an 80% prediction interval to determine whether these values may be used to determine concentration. Figure 7d shows corresponding positions of these data points for a selected trial at a sample concentration of 0.3 mg/mL (4.51 μM). For all three positions, the linear fit and prediction intervals show strong monotonic relationships between the absorbance metric value and the concentration. The statistical significance of the difference in absorbance was assessed using Welch's *t*-test, once for comparing the absorbances of the 0.10 and 0.15 mg/mL cases and another time for comparing the 0.15 and 0.30 mg/mL cases. With a chosen significance criterion of 0.05, the *t*-test was conducted with the null hypothesis that there is not a significant difference between two datasets. In both cases, the *p*-values output by the *t*-test (0.0024 and 0.0039, respectively) were significantly lower than the significance criteria. This allows us to reject the null hypothesis and confirm that there is a statistically significant difference between the absorbances of different concentrations. Furthermore, the second peak shows the strongest linear relationship, with a slope of 0.892 μM^{-1}, compared to slopes of the first peak and valley, respectively, 0.453 μM^{-1} and 0.515 μM^{-1}. For comparison, the premixed cases exhibited a slope of 0.616 μM^{-1} (Figure 3). Therefore, the second peak demonstrates the best sensitivity for a colorimetric assay.

Figure 8 shows the results for the case with the substrate heated to a temperature of 40 °C, compared to those at room temperature. A comparison of the timescales of the peaks and valleys demonstrate a dramatically increased rate of mixing (mixing time down from ∼200 to ∼125 s and reaction completion time down from ∼400 to ∼200 s) and, consequently, earlier completion of the reaction at a higher temperature. In our previous study of buoyancy-induced convection in droplets on nonwetting surfaces, Dash et al. demonstrated that mixing times on hydrophobic surfaces similar to those used in the current study are ∼15 times longer than that on superhydrophobic surfaces.[28] At a substrate temperature of 40 °C, the hydrophobic surface used here may be expected to exhibit a mixing time of ∼150 s, based on the mixing time of ∼10 s for superhydrophobic substrates.[28] For the heated substrate case in Figure 8, the mixing is complete at ∼125 s. Clearly, heating of the substrate is a viable method for dramatically speeding the time to measurement, as long as the denaturation temperature of the protein (60 °C[30]) is not reached. Furthermore, the volume of the droplet can be adjusted, with smaller volumes likely to result in faster mixing times. Given this reaction speed-up, along with the miniaturization of the measurement platform, droplet-based micromixing is demonstrated to be a viable alternative to microtiter plates for colorimetric measurements, which require longer or more complex mixing processes and complex fabrication.

DOI: 10.1021/acsomega.9b02784
ACS Omega 2019, 4, 22385−22391

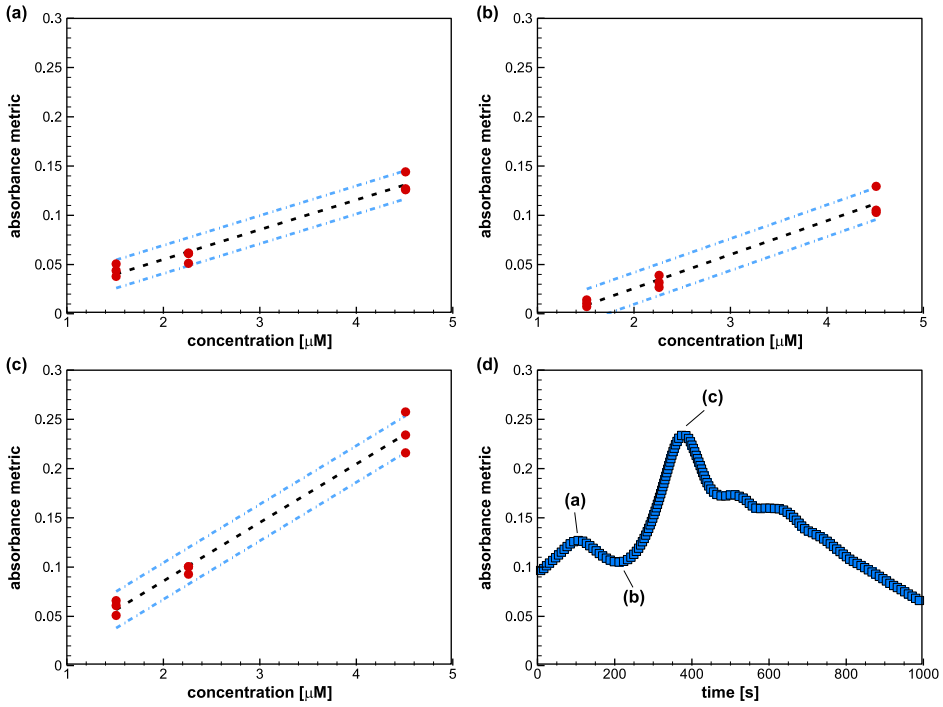

Figure 7. Absorbance metric is shown as a function of sample concentration at (a) the first peak, (b) the first valley, and (c) the second peak, along with their respective linear fits (dashed lines) and 80% prediction intervals (dash-dotted lines). The corresponding locations of the peaks and valleys in the temporal data are illustrated for one example trial in (d).

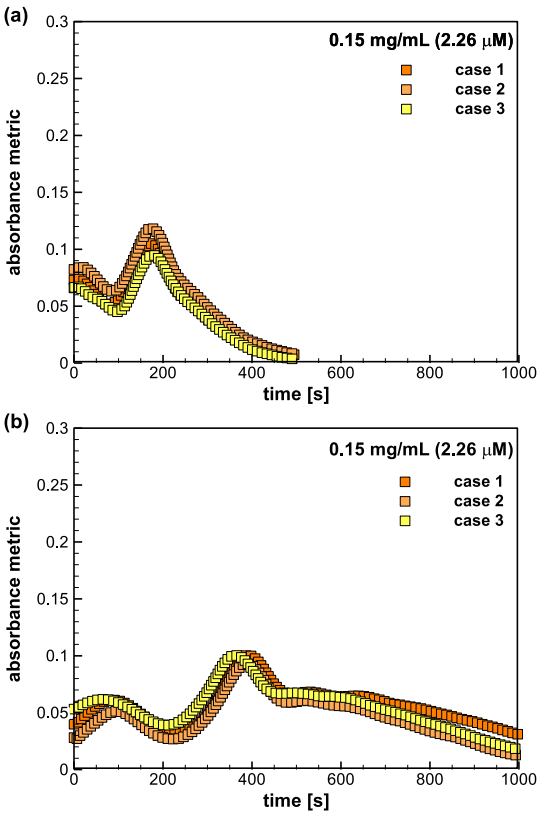

Figure 8. Time-resolved absorbance measurements for in situ mixed droplets at a sample concentration of 0.15 mg/mL (2.26 μM) for a substrate temperature of (a) 40 °C and (b) room temperature (21.5 °C).

4. CONCLUSIONS

Absorbance-based colorimetry is conducted using a sessile droplet on a nonwetting substrate. A discernible trend in the measured absorbance with sample concentration is first demonstrated in a sessile droplet for a case when the sample and reagent are premixed. The sample and reagent are then mixed in situ within a droplet, and the absorbance is measured in real time throughout the process. The measured temporal absorbance signal results from combined interactions between buoyancy-induced mixing, reaction between the sample and reagent, and adsorption of the protein molecules onto the nonwetting substrate. Analysis of videos of the reacting medium reveals the phases where each of these mechanisms dominates the trend in droplet absorbance. Statistical analysis of the absorbance data shows that the difference in signal between concentrations is statistically significant. The second transient peak in the absorbance measurement, associated with completion of the reaction, provides the highest sensitivity to sample concentration, and is therefore recommended for colorimetric quantitation during in situ mixing. Heating the substrate is shown to dramatically increase the rate of mixing, allowing for rapid concentration measurements. Overall, this sessile-droplet-based approach for absorbance-based colorimetry on a heated substrate provides a promising alternative to microwells for high-throughput parallel assays because of simple implementation and enhanced passive micromixing. Future work could involve optimization of surface modification, mixture ratios of the sample and reagent, and parallelization, in order to improve the efficiency of mixing, measurement accuracy, and device reusability.

DOI: 10.1021/acsomega.9b02784
ACS Omega 2019, 4, 22385−22391

■ ASSOCIATED CONTENT

Supporting Information

The Supporting Information is available free of charge at https://pubs.acs.org/doi/10.1021/acsomega.9b02784.

Data showing the volume and height evolution of the droplet during evaporation as well as the raw voltage signals for both the premixed cases and in situ mixed cases (PDF)

Video of 10 μL droplets on a nonwetting substrate with in situ mixing at a sample concentration of 0.3 mg/mL (4.51 μM) (MP4)

Video of 10 μL droplets on a nonwetting substrate with in situ mixing at a sample concentration of 2.0 mg/mL (30.01 μM) (MP4)

■ AUTHOR INFORMATION

Corresponding Author

*E-mail: sureshg@purdue.edu.

ORCID

Suresh V. Garimella: 0000-0003-1421-2912

Present Addresses

†Department of Chemical Engineering, Indian Institute of Technology Kharagpur.

‡Current President, University of Vermont.

Notes

The authors declare no competing financial interest.

■ REFERENCES

(1) King, E. J.; Garner, R. J. The Colorimetric Determination of Glucose. *J. Clin. Pathol.* **1947**, *1*, 30−33.

(2) Bradford, M. M. Rapid and Sensitive Method for the Quantitation of Microgram Quantities of Protein Utilizing the Principle of Protein-Dye Binding. *Anal. Biochem.* **1976**, *72*, 248−254.

(3) Lowry, O. H.; Rosebrough, N. J.; Farr, A. L.; Randall, R. J. Protein Measurement with the Folin Phenol Reagent. *J. Biol. Chem.* **1951**, *193*, 265−275.

(4) Smith, P. K.; Krohn, R. I.; Hermanson, G. T.; Mallia, A. K.; Gartner, F. H.; Provenzano, M. D.; Fujimoto, E. K.; Goeke, N. M.; Olson, B. J.; Klenk, D. C. Measurement of Protein Using Bicinchoninic Acid. *Anal. Biochem.* **1985**, *150*, 76−85.

(5) Duncombe, W. G. The Colorimetric Micro-Determination of Long-Chain Fatty Acids. *Biochem. J.* **1963**, *88*, 7−10.

(6) Burton, K. Study of the Conditions and Mechanism of the Diphenylamine Reaction for the Colorimetric Estimation of Deoxyribonucleic Acid. *Biochem. J.* **1956**, *62*, 315−323.

(7) Olson, B. J. S. C.; Markwell, J. Assays for Determination of Protein Concentration. *Curr. Protoc. Protein Sci.* **2007**, *48*, 3.4.1−3.4.29.

(8) Compton, S. J.; Jones, C. G. Mechanism of Dye Response and Interference in the Bradford Protein Assay. *Anal. Biochem.* **1985**, *151*, 369−374.

(9) Georgiou, C. D.; Grintzalis, K.; Zervoudakis, G.; Papapostolou, I. Mechanism of Coomassie Brilliant Blue G-250 Binding to Proteins: A Hydrophobic Assay for Nanogram Quantities of Proteins. *Anal. Bioanal. Chem.* **2008**, *391*, 391−403.

(10) Kruger, N. J. The Bradford Method For Protein Quantitation. In *The Protein Protocols Handbook*; Walker, J. M., Ed.; Springer Protocols Handbooks; Humana Press: Totowa, NJ, 2009; pp 17−24.

(11) Srinivasan, V.; Pamula, V. K.; Fair, R. B. An Integrated Digital Microfluidic Lab-on-a-Chip for Clinical Diagnostics on Human Physiological Fluids. *Lab Chip* **2004**, *4*, 310−315.

(12) Liu, S.; Su, W.; Ding, X. A Review on Microfluidic Paper-Based Analytical Devices for Glucose Detection. *Sensors* **2016**, *16*, 2086.

(13) Zhu, L.; Feng, Y.; Ye, X.; Feng, J.; Wu, Y.; Zhou, Z. An ELISA Chip Based on an EWOD Microfluidic Platform. *J. Adhes. Sci. Technol.* **2012**, *26*, 2113−2124.

(14) Yoon, J.-Y.; Garrell, R. L. Preventing Biomolecular Adsorption in Electrowetting-Based Biofluidic Chips. *Anal. Chem.* **2003**, *75*, 5097−5102.

(15) Pollack, M. G.; Shenderov, A. D.; Fair, R. B. Electrowetting-Based Actuation of Droplets for Integrated Microfluidics. *Lab Chip* **2002**, *2*, 96−101.

(16) Li, X.; Ballerini, D. R.; Shen, W. A Perspective on Paper-Based Microfluidics: Current Status and Future Trends. *Biomicrofluidics* **2012**, *6*, 011301.

(17) Hernandez-Perez, R.; Fan, Z. H.; Garcia-Cordero, J. L. Evaporation-Driven Bioassays in Suspended Droplets. *Anal. Chem.* **2016**, *88*, 7312−7317.

(18) Mayr, L. M.; Fuerst, P. The Future of High-Throughput Screening. *J. Biomol. Screening* **2008**, *13*, 443−448.

(19) Lye, J. K. K.; Ng, T. W.; Neild, A.; Liew, O. W. A Capacity for Mixing in Capillary Wells for Microplates. *Anal. Biochem.* **2011**, *410*, 152−154.

(20) Sarafoff, N. I.; Bieschke, J.; Giese, A.; Weber, P.; Bertsch, U.; Kretzschmar, H. A. Automated PrPres Amplification Using Indirect Sonication. *J. Biochem. Biophys. Methods* **2005**, *63*, 213−221.

(21) Oberti, S.; Neild, A.; Wah Ng, T. Microfluidic Mixing under Low Frequency Vibration. *Lab Chip* **2009**, *9*, 1435−1438.

(22) Yi, M.; Qian, S.; Bau, H. H. A Magnetohydrodynamic Chaotic Stirrer. *J. Fluid Mech.* **2002**, *468*, 153−177.

(23) Sadr, R.; Yoda, M.; Zheng, Z.; Conlisk, A. T. An Experimental Study of Electro-Osmotic Flow in Rectangular Microchannels. *J. Fluid Mech.* **2004**, *506*, 357−367.

(24) Schönfeld, F.; Hessel, V.; Hofmann, C. An Optimised Split-and-Recombine Micro-Mixer with Uniform 'Chaotic' Mixing. *Lab Chip* **2004**, *4*, 65−69.

(25) Dash, S.; Garimella, S. V. Droplet Evaporation Dynamics on a Superhydrophobic Surface with Negligible Hysteresis. *Langmuir* **2013**, *29*, 10785−10795.

(26) Pan, Z.; Dash, S.; Weibel, J. A.; Garimella, S. V. Assessment of Water Droplet Evaporation Mechanisms on Hydrophobic and Superhydrophobic Substrates. *Langmuir* **2013**, *29*, 15831−15841.

(27) Chandramohan, A.; Weibel, J. A.; Garimella, S. V. Spatiotemporal Infrared Measurement of Interface Temperatures during Water Droplet Evaporation on a Nonwetting Substrate. *Appl. Phys. Lett.* **2017**, *110*, 041605.

(28) Dash, S.; Chandramohan, A.; Weibel, J. A.; Garimella, S. V. Buoyancy-Induced on-the-Spot Mixing in Droplets Evaporating on Nonwetting Surfaces. *Phys. Rev. E* **2014**, *90*, 062407.

(29) Deegan, R. D.; Bakajin, O.; Dupont, T. F.; Huber, G.; Nagel, S. R.; Witten, T. A. Capillary Flow as the Cause of Ring Stains from Dried Liquid Drops. *Nature* **1997**, *389*, 827−829.

(30) Borzova, V. A.; Markossian, K. A.; Chebotareva, N. A.; Kleymenov, S. Y.; Poliansky, N. B.; Muranov, K. O.; Stein-Margolina, V. A.; Shubin, V. V.; Markov, D. I.; Kurganov, B. I. Kinetics of Thermal Denaturation and Aggregation of Bovine Serum Albumin. *PLoS One* **2016**, *11*, No. e0153495.

DOI: 10.1021/acsomega.9b02784
ACS Omega 2019, 4, 22385−22391